Materials Science & Engineering A 832 (2022) 142388

Contents lists available at ScienceDirect

Materials Science & Engineering A

journal homepage: www.elsevier.com/locate/msea

Suppression of abnormal grain growth in friction-stir welded aluminum by pre-strain rolling: Limitation of the approach

Alexander Kalinenko, Igor Vysotskiy, Sergey Malopheyev, Marat Gazizov, Sergey Mironov *, Rustam Kaibyshev

Belgorod National Research University, Pobeda 85, Belgorod, 308015, Russia

ARTICLE INFO

Keywords:
Aluminium alloys
Friction-stir welding
Abnormal grain growth
Microstructure-strength relationship
Electron backscatter diffraction (EBSD)

ABSTRACT

This work emphasizes the limited efficiency of the pre-straining approach for suppression of abnormal grain growth in friction-stir welds produced at low-heat-input conditions. In this case, the introduced dislocation density is insufficient to overbalance grain-boundary energy. Hence, the subsequent annealing behavior is governed by the grain growth rather than recrystallization.

1. Introduction

The relatively low stability of welded materials against abnormal grain growth is often considered a significant problem in friction-stir welding/processing (FSW/P) of aluminum alloys [1,2]. This phenomenon typically occurs during either post-weld solutionizing treatment or superplastic deformation and involves a catastrophic coarsening of a few grains which rapidly consume the almost entire weld zone [2–7]. This undesirable effect is usually explained in terms of the cellular Humphreys' theory [8] being attributed to a synergetic effect of grain refinement and dissolution of second-phase particles [e.g. 2, 3].

Recently, the pre-strain rolling approach has been proposed to suppress the abnormal grain growth in friction-stirred materials [9]. This technique implied cold rolling of the as-welded material to a relatively small plastic strain with the aim to introduce high density of tangled dislocations. This should provide a driving force for recrystallization during subsequent annealing and thus avoid the abnormal microstructural coarsening.

It should be stressed that the above approach is effective only if the driving force for the recrystallization process is essentially higher than that for the grain growth, i.e., if the energy stored in dislocations is significantly larger than the total grain-boundary energy. In this context, it is worth noting that the grain-boundary energy increases with grain refinement. Considering the mean grain size of ~1 μm (i.e., a typical grain structure produced during low-temperature FSW) and taking the typical magnitudes of grain-boundary energy for aluminum, it can be shown that the required dislocation density exceeds 10^{15} m^{-2}. This value seems to be excessively high. Therefore, the feasibility of the pre-strain approach for the fine-grained aluminum is not obvious.

Therefore, the purpose of the present study was the evaluation of the efficiency of this technique in the case of a typical low-heat-input friction-stir weld.

2. Experimental

To maintain consistency with the original paper, which invented the pre-strain rolling approach [9], the same program material (i.e., commercial 6061 aluminum alloy), was used in the present study. The received hot-extruded bar was undergone T6 tempering treatment, i.e., solution annealed at 540 °C for 1 h, water quenched, and then aged at 160 °C for 8 h. This material condition was denoted as *base material*.

The 3-mm-thick sheets of the base material were butt-welded using the commercial AccurStir FSW machine. The welding tool had a conventional design consisting of a concave-shaped shoulder of 12.5 mm in diameter, and a threaded M5 cylindrical probe of 2.7 mm in length. To produce the fine-grained microstructure in the stir zone, the relatively low heat-input FSW conditions were used in the present study. Based on the previous work [10], those included the spindle rate of 500 rpm and the feed rate of 380 mm/min, and provided the peak temperature in the stir zone of ≈370 °C. Further welding details have been reported elsewhere [11]. The typical conventions of FSW geometry were used with WD, ND, and TD being the welding direction, normal direction, and

* Corresponding author.
E-mail address: mironov@bsu.edu.ru (S. Mironov).

https://doi.org/10.1016/j.msea.2021.142388
Received 4 October 2021; Received in revised form 14 November 2021; Accepted 22 November 2021
Available online 24 November 2021

transverse direction, respectively.

To examine thermal stability of the produced welds, those were subjected to the T6 tempering treatment in the manner described above. In order to evaluate the efficiency of the pre-strain approach, selected welds were cold-rolled prior to the post-weld heat treatment. The rolling was conducted along the TD to the total thickness reduction of 10%.

Microstructural observations were conducted using electron backscatter diffraction (EBSD) and transmission electron microscopy (TEM). In all cases, a suitable surface finish was obtained by electro-polishing in a solution of 25% nitric acid in methanol. EBSD was performed with an FEI Quanta 600 field-emission-gun scanning electron microscope equipped with TSL OIM™ system and operated at 20 kV. Depending on the scale of a particular microstructure, the scan step size was varied from 0.2 to 5 μm. A 15-degree criterion was used to differentiate low-angle boundaries (LABs) from high-angle boundaries (HABs). Grain size was quantified by applying the grain-reconstruction approach [12], i.e., considering each grain in an EBSD map as a circle with equivalent area and calculating the associated circle-equivalent diameter. TEM observations were conducted with JEOL JEM-2100EX transmission electron microscope operated at 200 kV. Dislocation density was measured employing the linear intercept approach.

Mechanical properties of the welded joints were examined using microhardness measurements and transverse tensile tests. Vickers microhardness profiles were acquired across the weld mid-thickness by applying a load of 200 g and a dwell time of 10 s. The tensile tests were performed according to ASTM E8M standard. The tensile specimens were machined perpendicular to the WD, were centered along the weld line, and had a gauge section of 26 mm in length and 6 mm in width. The upper and bottom surfaces of the specimens were mechanically polished to achieve uniform thickness and remove the kissing bond defect. The tension tests to failure were conducted using an Instron 5882 universal testing machine at room temperature and the nominal strain rate of 10^{-3} s^{-1}. Two tensile specimens were tested for each material condition. To provide additional insight into the tensile behavior, the in-plane strain distributions were measured using a commercial Vic-3D digital image correlation system.

3. Results

3.1. Microstructural observations

The influence of the pre-strain cold rolling on the stir zone microstructure is shown in Fig. 1. In the as-welded condition, the microstructure was dominated by the fine equiaxed grains which contained a developed LAB substructure (Fig. 1a). Such microstructures are typically found in aluminum friction-stir welds, being typically attributed to the continuous recrystallization operating during FSW [e.g. 13]. In the present study, the mean HAB intercept was measured to be ≈ 2 μm. Importantly, the dislocation density in the as-FSWed state was very low (Fig. 1b). The subsequent cold rolling provided significant changes in neither grain size nor grain shape but increased the dislocation density up to 5×10^{13} m^{-2} (Fig. 1c). Remarkably, the dislocations were found to be arranged into a poorly-developed cell structure (Fig. 1c).

The microstructural changes induced during subsequent heat treatment are summarized in Figs. 2 and 3. Specifically, Fig. 2 shows the sample-scale EBSD maps taken from the entire weld zone in different material conditions, viz. (i) in the as-FSWed state (Fig. 2a), (ii) after FSW and the post-weld T6 tempering treatment (Fig. 2b), and (iii) after FSW, the subsequent cold rolling, and the T6 treatment (Fig. 2c).

In the conventional process, which involved no pre-strain rolling, T6 tempering resulted in considerable microstructural coarsening in the stir zone (compare Fig. 2a and b). As shown in the previous work [14], the annealed material exhibited bimodal grain-size distribution thus evidencing the abnormal mechanism of the grain growth. It is interesting to note that the microstructural coarsening developed heterogeneously across the stir zone. Specifically, the relatively fine-grained layer has retained on its retreating side (dotted line in Fig. 2b). This phenomenon is thought to originate from the static recrystallization occurring in the thermo-mechanical affected zone (TMAZ) during solution annealing [14].

The pre-strain rolling resulted in some reduction of the final grain size in the T6-tempered condition (Fig. 3) but could not suppress the abnormal grain growth completely (Fig. 2c). This result appears to indicate a relatively low efficiency of the pre-strain approach, thus being in the line with the main idea of the present study. It is also worth noting that the fine-grained layer at the retreating side of the stir zone had survived in the pre-strained material (dotted line in Fig. 2c).

3.2. Microhardness

The effect of the post-weld treatments on the microhardness profile is shown in Fig. 4a. For simplicity, the diameter of the tool probe (which virtually coincides with the size of the stir zone) is indicated in the figure. In the as-welded condition, a substantial material softening was found in the stir zone. Considering the relatively low welding temperature, this effect was mainly associated with the coarsening of secondary precipitates [7].

As expected, the post-weld rolling resulted in material hardening but this effect was not very high (Fig. 4a). However, the following T6 tempering had recovered material strength almost completely thus producing a nearly-flat microhardness distribution (Fig. 4a). This effect is well described in scientific literature being usually attributed to the homogeneous precipitation of strengthening dispersoids.

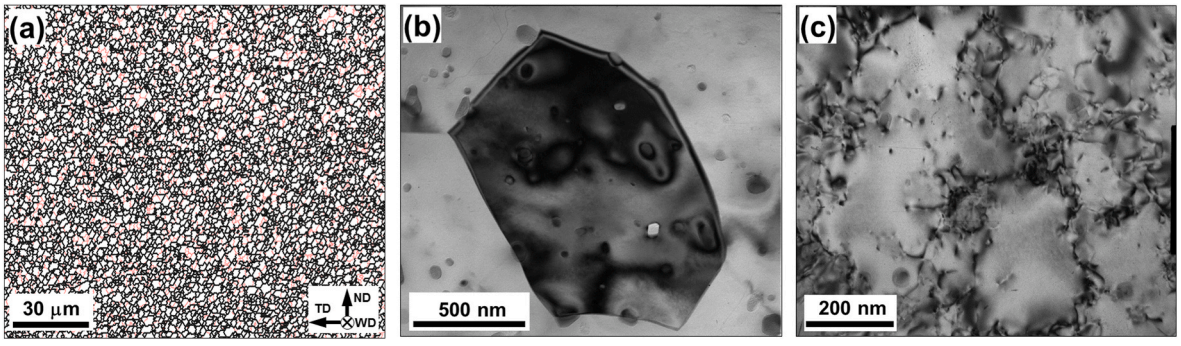

Fig. 1. Microstructure of the stir zone in the as-FSWed condition: (a) EBSD map, and (b) TEM image, and (c) TEM micrograph showing typical dislocation structure produced in the stir zone after cold rolling. In (a), LABs and HABs are depicted as red lines and black lines, respectively; WD, ND, and TD are welding direction, normal direction, and transverse direction, respectively. (For interpretation of the references to color in this figure legend, the reader is referred to the Web version of this article.)

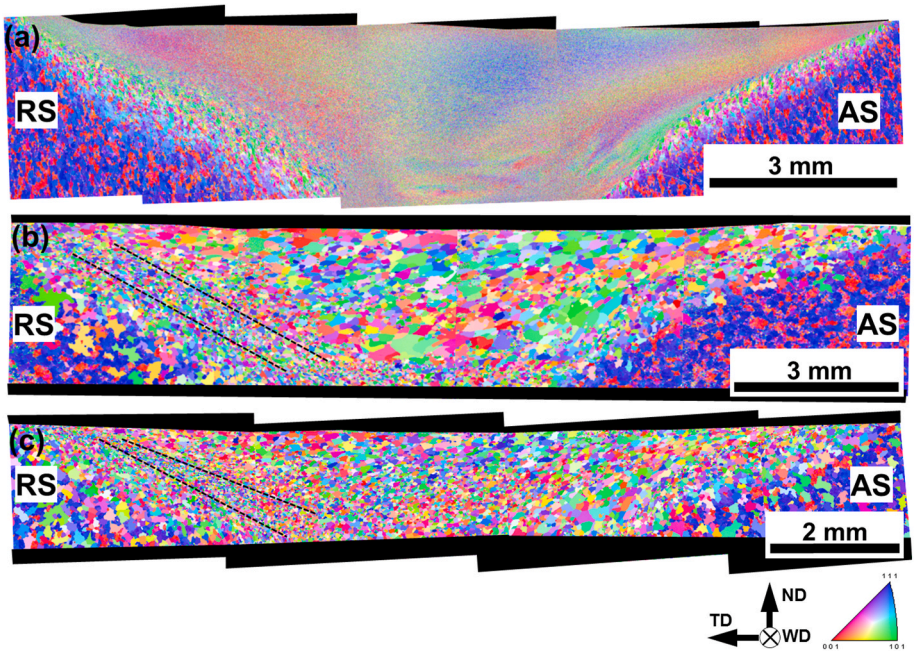

Fig. 2. Sample-scale EBSD maps taken from the welded material (a) in the as-FSWed condition, (b) after FSW and the post-weld T6 tempering treatment, and (c) after FSW, subsequent cold rolling, and T6 tempering treatment. In the maps, grains are colored according to their crystallographic orientations relative to the WD. The color code triangle and reference frame for EBSD maps are shown in the bottom right corner. In (b) and (c), dotted lines indicate the fine grained layer at the edge of the stir zone. In all cases, RS is retreating side and AS is advancing side. WD, ND, and TD are welding direction, normal direction, and transverse direction, respectively. (For interpretation of the references to color in this figure legend, the reader is referred to the Web version of this article.)

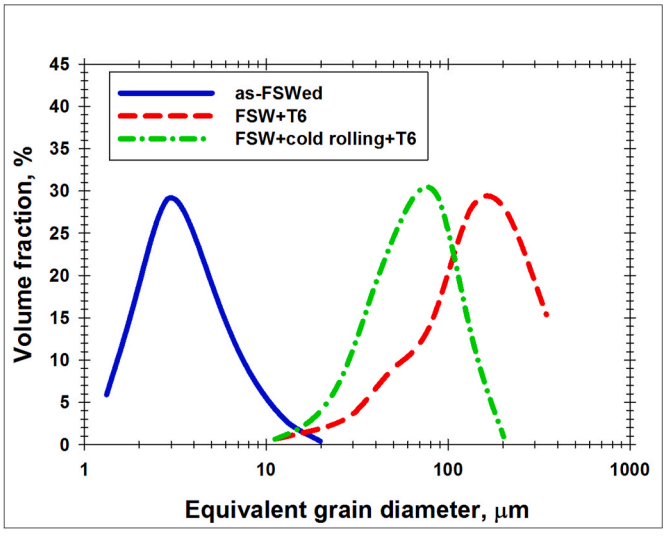

Fig. 3. Effect of the post-weld thermo-mechanical treatment on grain-size distribution in the central section of the stir zone.

3.3. Tensile behavior

The tensile behavior of the welds in different processing conditions is shown in Fig. 4b. As expected, FSW led to significant degradation of both the strength and ductility. In the previous work [7], the latter result was attributed to the localization of the tensile strain in the softened stir zone.

The post-weld T6 treatment has restored mechanical strength but weld ductility was still relatively low (Fig. 4b). In the conventional process (which involved no pre-strain rolling), this effect was associated with the abnormal grain growth in the stir zone. It has been shown recently [14] that the relatively high strain hardening rate, which is inherent to the coarse-grained materials, tended to suppress the tensile strain in the stir zone. As a result, it was preferentially concentrated in the fine-grained TMAZ, and thus the global elongation-to-failure was comparatively small.

The pre-strain rolling has improved the weld ductility but it was still lower than that of the base material (Fig. 4b). In order to get a closer inspection of the tensile behavior of the pre-strained material, the digital-image-correlation technique was employed, with the typical results being shown in Fig. 5. It was found that the distribution of the tensile strain was still inhomogeneous, with the peak strain being clustered at the retreating side of the stir zone. From a comparison of the strain distributions with the sample-scale EBSD map in Fig. 2c, it seems that the tensile strain still tended to concentrate in the fine-grained TMAZ.

It is worth noting that investigation of the influence of the abnormal-coarse grains on other mechanical properties (including fatigue strength, fracture toughness, bending behavior, etc.) also represents an essential interest. However, this issue is outside the scope of the present study.

4. Discussion

From experimental observations, it is clear that the pre-strain rolling had not suppressed the abnormal grain growth completely. Hence, the microstructure evolved after subsequent T6 tempering was not totally homogeneous, and thus the tensile behavior of the tempered welds was not entirely uniform.

To comprehend the insufficient effectiveness of the pre-straining approach, it is necessary to interpret the annealing behavior of the pre-processed material. To this end, the total grain boundary energy was compared with the total dislocation energy. The grain-boundary energy is usually evaluated as $E_{GB} = 3\gamma/d$, where γ is the specific grain-boundary energy (=0.324 J/m), and d is the mean grain size ($=2\times10^{-6}$ m). On the other hand, the total dislocation energy is typically calculated as $E_d = 0.5Gb^2\rho$, where G is shear modulus ($=2.4\times10^{10}$ N/m^2), b is the Burgers vector ($=0.286\times10^{-9}$ m), and ρ is dislocation density ($=5\times10^{13}$ m^{-2}).

From calculations, the energy stored in grain boundaries ($\approx4.9\times10^5$ N/m^2) was essentially larger than the dislocation energy ($\approx0.5\times10^5$ N/m^2). Hence, the driving force for recrystallization was relatively low. Therefore the microstructural coarsening during subsequent T6 tempering was primarily governed by the grain growth. Taking into account the comparatively small final grain size in the fully-annealed condition (Fig. 3), the pre-straining had obviously exerted an

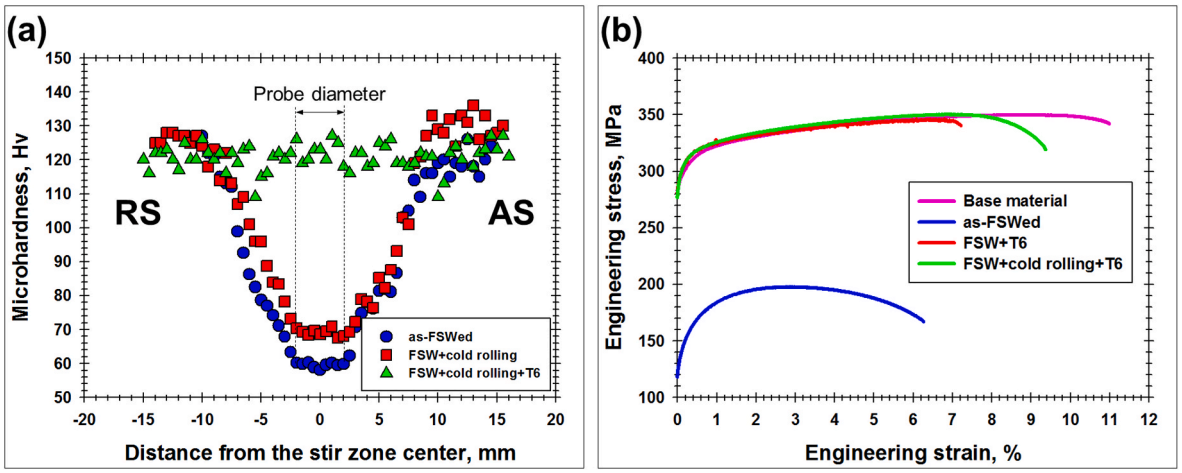

Fig. 4. Effect of the post-weld thermo-mechanical treatment on (a) microhardness profile and (b) tensile diagrams. In (a), RS and AS are retreating side and advancing side, respectively.

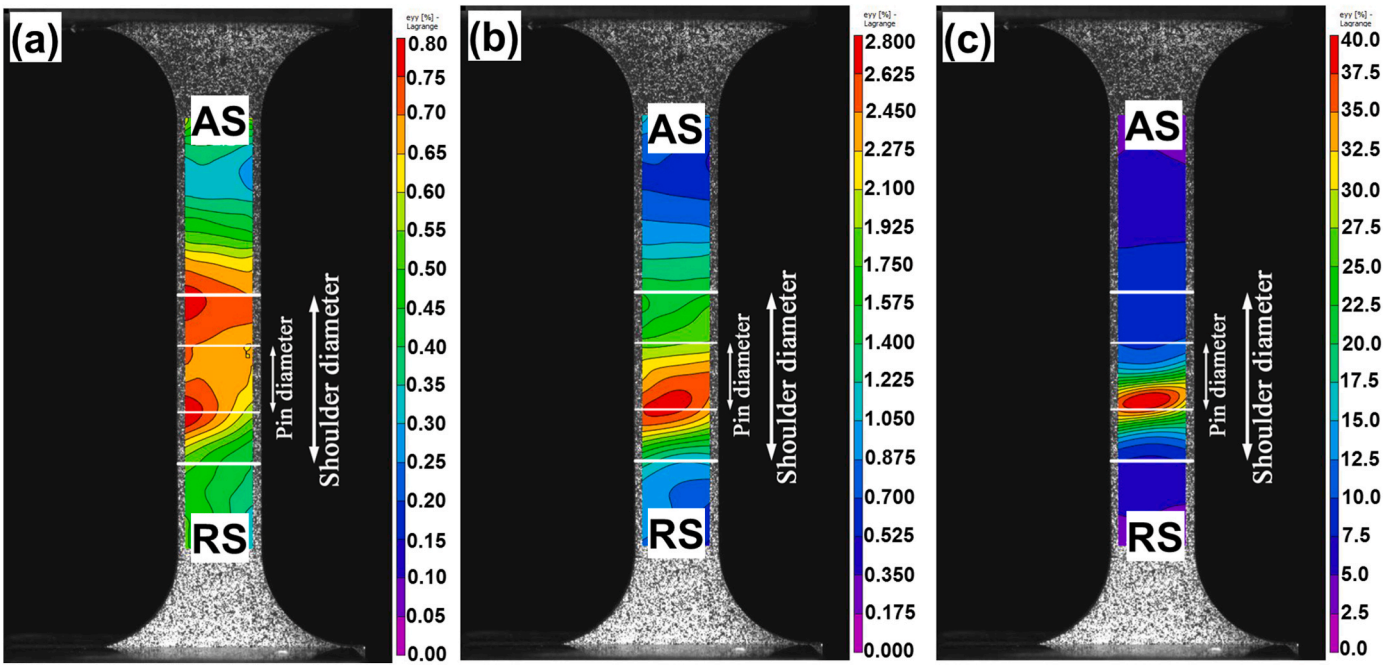

Fig. 5. The distribution of longitudinal strains evolved during transverse tensile tests of the welded specimens subjected to the post-weld cold-rolling and subsequent T6 tempering treatment after a global tensile strain of (a) 0.2%, (b) 1.0%, and (c) immediately before failure. RS and AS are retreating side and advancing side, respectively.

influence on the annealing behavior. Nevertheless, it was insufficient to suppress the abnormal grain growth completely.

From a broad perspective, the dislocation density (i.e., the recrystallization driving force) can be enhanced by increasing the rolling strain. This, however, may lead to the unacceptable change of the weld thickness. Moreover, this may also result in a formation of the dislocation cell structure which should partially relax the dislocation energy. The first evidence of this process was seen even at the relatively low dislocation density achieved in the present study (Fig. 1c). Obviously, this phenomenon should become more pronounced at higher plastic strains.

5. Conclusions

This work was undertaken to evaluate the feasibility of the pre-straining approach for suppression of the abnormal grain growth in the fine-grained friction-stir welds. It was found that the dislocation density introduced during the pre-strain rolling was insufficient to overbalance the grain-boundary energy. Accordingly, the microstructural evolution during subsequent solution annealing was governed primarily by the grain growth mechanism. Therefore, the pre-straining approach appears to be not effective for suppression of the abnormal grain growth in the fine-grained aluminum friction-stir welds.

Data availability

The raw/processed data required to reproduce these findings cannot be shared at this time as the data also forms part of an ongoing study.

Originality statement

I write on behalf of myself and all co-authors to confirm that the

results reported in the manuscript are original and neither the entire work, nor any of its parts have been previously published. The authors confirm that the article has not been submitted to peer review, nor has been accepted for publishing in another journal. The authors confirm that the research in their work is original, and that all the data given in the article are real and authentic. If necessary, the article can be recalled, and errors corrected.

CRediT authorship contribution statement

Alexander Kalinenko: Conceptualization, Investigation, Methodology, Writing – review & editing. **Igor Vysotskiy:** Investigation, Methodology, Writing – review & editing. **Sergey Malopheyev:** Investigation, Methodology, Writing – review & editing. **Marat Gazizov:** Investigation, Writing – review & editing. **Sergey Mironov:** Conceptualization, Funding acquisition, Project administration, Data curation, Formal analysis, Investigation, Software, Validation, Visualization, Writing – original draft. **Rustam Kaibyshev:** Conceptualization, Supervision, Writing – review & editing.

Declaration of competing interest

The authors declare that they have no known competing financial interests or personal relationships that could have appeared to influence the work reported in this paper.

Acknowledgments

This study was financially supported by the Russian Science Foundation (grant No. 19-49-02001). The authors are also grateful to the personnel of the Joint Research Center “Technology and Materials” at Belgorod State National Research University for experimental assistance.

References

[1] R.S. Mishra, Z.Y. Ma, Friction stir welding and processing, Mater. Sci. Eng. R 50 (2005) 1–78, https://doi.org/10.1016/j.mser.2005.07.001.

[2] I. Charit, R.S. Mishra, Abnormal grain growth in friction stir processed alloys, Scripta Mater. 58 (2008) 367–371, https://doi.org/10.1016/j.scriptamat.2007.09.052.

[3] KhA.A. Hassan, A.F. Norman, D.A. Price, P.B. Prangnell, Stability of nugget zone grain structure in high strength Al-alloy friction stir welds during solution treatment, Acta Mater. 57 (2003) 1923–1936, https://doi.org/10.1016/S1359-6454(02)00598-0.

[4] I.S. Zuiko, S. Mironov, S. Betsofen, R. Kaibyshev, Suppression of abnormal grain growth in friction-stir welded Al–Cu–Mg alloy by lowering of welding temperature, Scripta Mater. 196 (2021) 113765, https://doi.org/10.1016/j.scriptamat.2021.113765.

[5] M.B. Lezaack, A. Simar, Avoiding abnormal grain growth in thick 7XXX aluminium alloy friction stir welds during T6 post heat treatments, Mater. Sci. Eng., A 807 (2021) 140901, https://doi.org/10.1016/j.msea.2021.140901.

[6] P. Nelaturu, S. Jana, R.S. Mishra, G. Grant, B.E. Carlson, Effect of temperature on the fatigue cracking mechanisms in A356 Al alloy, Mater. Sci. Eng., A 780 (2020) 139175, https://doi.org/10.1016/j.msea.2020.139175.

[7] A. Kalinenko, I. Vysotskiy, S. Malopheyev, S. Mironov, R. Kaibyshev, New insight into the phenomenon of the abnormal grain growth in friction-stir welded aluminum, Mater. Lett. 302 (2021) 130407, https://doi.org/10.1016/j.matlet.2021.130407.

[8] F.J. Humphreys, A unified theory of recovery, recrystallization and grain growth, based on the stability and growth of cellular microstructures—II. The effect of second-phase particles, Acta Mater. 45 (1997) 5031–5039.

[9] I. Vysotskiy, S. Malopheyev, S. Mironov, R. Kaibyshev, Pre-strain rolling as an effective tool for suppression of abnormal grain growth in friction-stir welded 6061 aluminum alloy, Mater. Sci. Eng., A 733 (2018) 39–42, https://doi.org/10.1016/j.msea.2018.07.026.

[10] A. Kalinenko, I. Vysotskiy, S. Malopheyev, S. Mironov, R. Kaibyshev, Influence of the weld thermal cycle on the grain structure of friction-stir joined 6061 aluminum alloy, Mater. Char. 178 (2021) 111202, https://doi.org/10.1016/j.matchar.2021.111202.

[11] A. Kalinenko, K. Kim, I. Vysotskiy, I. Zuiko, S. Malopheyev, S. Mironov, R. Kaibyshev, Microstructure-strength relationship in friction-stir welded 6061-T6 aluminum alloy, Mater. Sci. Eng., A 793 (2020) 139858, https://doi.org/10.1016/j.msea.2020.139858.

[12] F.J. Humphreys, Quantitative metallography by electron backscatter diffraction, J. Microsc. 195 (1999) 170–185, https://doi.org/10.1046/j.1365-2818.1999.00578x.

[13] R.W. Fonda, J.F. Bingert, K.J. Colligan, Development of grain structure during friction stir welding, Scripta Mater. 51 (2004) 243–248, https://doi.org/10.1016/j.scriptamat.2004.04.017.

[14] A. Kalinenko, I. Vysotskii, S. Malopheyev, S. Mironov, R. Kaibyshev, Relationship between welding conditions, abnormal grain growth and mechanical performance in friction-stir welded 6061-T6 aluminum alloy, Mater. Sci. Eng., A 817 (2021) 141409, https://doi.org/10.1016/j.msea.2021.141409.